Optics Letters

Machine learning-based pulse characterization in figure-eight mode-locked lasers

Alexey Kokhanovskiy,[1,*] Anastasia Bednyakova,[1,2] Evgeny Kuprikov,[1] Aleksey Ivanenko,[1] Mikhail Dyatlov,[1] Daniil Lotkov,[1] Sergey Kobtsev,[1] and Sergey Turitsyn[1,3]

[1]Division of Laser Physics and Innovative Technologies, Novosibirsk State University, Pirogova str., 2, Novosibirsk, 630090, Russia
[2]Institute of Computational Technologies SB RAS, Novosibirsk, 630090, Russia
[3]Aston Institute of Photonic Technologies, Aston University, B4 7ET, Birmingham, UK
*Corresponding author: alexey.kokhanovskiy@gmail.com

Received 16 May 2019; revised 11 June 2019; accepted 11 June 2019; posted 12 June 2019 (Doc. ID 367781); published 1 July 2019

By combining machine learning methods and the dispersive Fourier transform we demonstrate, to the best of our knowledge, for the first time the possibility to determine the temporal duration of picosecond-scale laser pulses using a nanosecond photodetector. A fiber figure of eight lasers with two amplifiers in a resonator was used to generate pulses with durations varying from 28 to 160 ps and spectral widths varied in the range of 0.75–12 nm. The average power of the pulses was in the range from 40 to 300 mW. The trained artificial neural network makes it possible to predict the pulse duration with the mean agreement of 95%. The proposed technique paves the way to creating compact and low-cost feedback for complex laser systems.

https://doi.org/10.1364/OL.44.003410

One of the modern trends in the development of mode-locked fiber lasers is a focus on precise adjustment of temporal and spectral properties of optical pulses [1–4] at the expense of the increasing complexity of the system design. The resulting large number of cavity parameters defining the laser performance requires new approaches to controlling them. From this view point, the machine learning-based techniques are attractive for control and management of complex laser systems. Machine learning algorithms have already been used for optimization of the laser performance [5], self-starting [6], and adjustment of system parameters to environmental changes [7].

A key part of any self-adjusting laser system is a feedback loop which links the laser performance and variable laser cavity parameters. In general, experimental realization of such feedback system requires a set of measurement devices and (desirably) electronically controlled feedback to laser cavity parameters. To optimize the performance of an electronically controlled mode-locked fiber laser based on nonlinear polarization evolution, four devices were used: an autocorrelator, optical and radio-frequency (RF) analyzers, and an oscilloscope [5,6]. In a fiber laser with a spatial light modulator, the autocorrelator and optical analyzer formed a feedback system to generate 40 fs pulses [1]. The laser performance also could be optimized outside its cavity, for example, by a pulse compressor that requires a frequency-resolved optical gating measurement as a feedback response [8]. To sum up, the common way to create a feedback for adaptive fiber lasers is to use an optical spectrum analyzer, oscilloscope, and autocorrelator (or other device measuring the duration of ultra-short pulses) as measurement setups. These devices provide information about basic pulse parameters: optical spectrum, time duration, repetition rate, average power, and peak power. In principle, the pulse has to be measured in both time and frequency domains because of the nontrivial relation between the optical spectrum and time envelope of the pulse [9].

A large set of tools leads to the complexity and corresponding cost of the controlled devices that greatly limit the application of the emerging feedback-based approaches to laboratory experiments. A reduction in the number of measurement tools and devices required for the realization of a feedback loop is a critical challenge in the development of "smart" laser systems. In a broader perspective, the first attempt to reduce the number of measurement setups was made in Ref. [10], where neural network predicts pulse parameters of an x-ray-free electron laser.

The novelty of this Letter is an experimental demonstration of a feedback system that requires a nanosecond detector to measure all listed basic parameters of a picosecond pulse. We implement this novel technique using the following steps using acquisition of an oscilloscope trace. First, the registration of a time-domain comb of pulses indicates the mode-locking regime. Secondly, the Fourier transform of an oscilloscope trace provides information about the RF spectrum of the mode-locked regime and, consequently, about a quality of mode locking. Finally, dispersive Fourier transform (DFT) analysis available from the oscilloscope trace of dispersively stretched pulses, allows one to measure optical spectrum of the pulses [11]. We would like to stress that an oscilloscope trace of short optical pulses does not give directly any information about their duration. The sensitivity of the photodetector is limited by its relaxation time, which makes it impossible to measure the duration of optical pulses less than hundreds of picoseconds.

The goal of this Letter is to demonstrate a feasibility of measurement of the temporal characteristics of the output pulses of a figure of eight (F-8) fiber laser employing a DFT trace of the pulse comb and machine learning technique. To determine the temporal width of the pulses, we used machine learning techniques focusing on an artificial neural network (ANN). We demonstrate the general approach using as an example the F-8 fiber lasers with two amplifiers, where a large number of pulse regimes with different spectral and temporal characteristics can be observed. We believe that our findings pave the way to implement a compact and relatively low-cost feedback loop for laser systems.

Figure 1(a) illustrates the F-8 mode-locked fiber laser under study. The laser cavity consists of two fiber loops, unidirectional (main) and bidirectional (nonlinear amplifying loop mirror) ones, connected to each other by a 40/60 coupler. The main loop includes 70% output coupler and a high-power Faraday isolator that provides unidirectional propagation. Both loops compose 2.5 m long amplifying sections of double-clad Yb-doped fibers with the absorption of 3.9 dB/m at 978 nm. The active fibers are pumped through fiber beam combiners by independently controlled multimode laser diodes with an optical power of up to 4.5 W at a wavelength of 978 nm. The fibers inside the cavity, both passive and active, are polarization-maintaining.

To measure the basic parameters of the mode-locked pulse such as time duration, the optical spectrum, and the RF spectrum, the following tools were used: the A.P.E. pulseCheck autocorrelator with a scanning range from 120 fs up to 160 ps, Tektronix RSA 3308B RF spectrum analyzer with 2 Hz resolution for inter-mode beat signal measuring, the Yokogawa AQ 6375 optical spectrum analyzer (OSA) with resolution 0.1 nm, and the Tektronix DPO71604C oscilloscope connected with a photodetector with a bandwidth of 1 GHz.

A full width at half-maximum (FWHM) of the autocorrelation function (ACF) was used as a measure of pulse duration. The ACF duration of generated pulses varied from 28 to 160 ps. To distinguish single-scale (coherent) and double-scale (noise-like) pulses, we also measure a contrast of the ACF coherence spike [Fig. 1(b)]. The contrast of the coherence spike was calculated as the difference between a height of coherence spike and a height of the ACF envelope of a normalized ACF trace. To derive the height of the ACF envelope, we applied to the ACF trace the low-pass three-order Butterworth filter with 0.01 (π rad/sample) cutoff frequency. For example, the contrast of the ACF coherence spike of a noise-like pulse shown in Fig. 1(b) (green line) is 0.32. The contrast of the coherence spike varied from 0.0036 to 0.5. We assume that noise-like pulses have coherence spike contrast higher than 0.02. Optical spectrum of mode-locked pulses generated by the fiber laser includes two parts, corresponding to a signal pulse and noisy Raman pulse [Fig. 1(c)]. Both pulses were characterized by the average power and spectrum width. For the signal part,

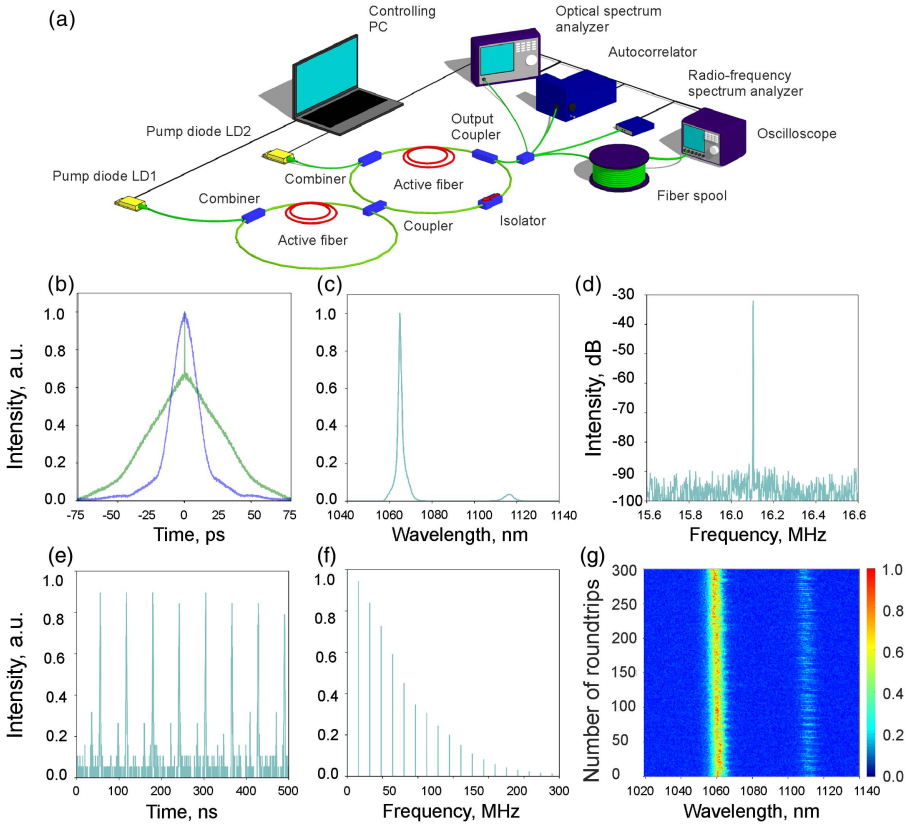

Fig. 1. (a) Experimental setup. (b) ACF examples of coherent (blue line) and noise-like (green line) output pulses. (c) Example of the optical spectrum of a pulse with a significant Raman part. (d) Example of an RF spectrum of a pulse comb near the fundamental mode of a laser cavity. (e) Oscilloscope trace of a pulse comb detected after propagation through a long spool of a fiber. (f) Fourier transformation of an oscilloscope trace representing the RF spectrum of the DFT pulse comb. (g) DFT of a pulse comb presenting the optical spectrum of a pulse per roundtrip.

these values ranged between 40 and 300 mW and 0.75 and 12 nm, respectively. The average power of the Raman ranged between 0 and 35% of total power. The signal-to-noise ratio of RF inter-mode beats (RF contrast in RF maps) was measured as a contrast between the background level and the spike at fundamental frequency [Fig. 1(d)]. The RF contrast varied between 0 and 73 dB.

In this Letter, we aim to replace these three measurement tools by a single oscilloscope that measures the DFT trace of optical pulses. To measure the DFT trace of optical pulses, we used a 14.93 km long fiber span with dispersion $\beta_2 = 15.1\text{e-}27\ s^2/m$. Stretched pulses were measured by the oscilloscope with the sampling rate of 3 GS/s [Fig. 1(e)]. Some pulse parameters such as RF and optical spectrum can be measured directly from the DFT trace. The Fourier transformation of the DFT trace gives the RF spectrum of a pulse comb [Fig. 1(f)]. Using the obtained RF spectrum, we calculated the number, average power, and standard deviation of the RF peaks. Rescaling the DFT trace provides the optical spectrum of pulses per roundtrip [Fig. 1(g)] and, therefore, gives information similar to the OSA.

The most challenging part was to determine the temporal duration of a pulse. In fact, there is no direct relation between its optical or RF spectrum and time duration. However, a laser system with specific chromatic dispersion, nonlinear coefficient, and Stokes shift generates a specific set of pulsed regimes and, therefore, there is no need to make a universal measurement tool to determine pulse parameters. In this Letter, we demonstrate that it is possible to train an ANN to determine with acceptable accuracy a temporal duration of the pulses by following the features extracted from the DFT trace: (1) optical spectral width of signal, (2) optical spectral width of Raman pulse, (3) optical power of signal, (4) optical power of a Raman pulse, (5) total optical power, (6) number of RF spectrum peaks, (7) average power of RF spectrum peaks, and (8) standard deviation (std) of the RF peak power.

It is worth mentioning that direct measuring of an optical spectrum of a pulse using a DFT setup requires careful adjusting of the input power to reduce the influence of nonlinear effects such as self-phase modulation and Raman scattering. We would have to implement a variable attenuator to control the input power and measure the optical spectrum width of the pulses with average powers from 40 to 300 mW. Instead of using an attenuator, we apply an ANN to predict a width of an optical spectrum at the laser output, assuming nonlinear dependency between the spectra width at the DFT line input and output.

At the first stage, we estimate and ACF width for the whole variety of generated optical pulses, including partially coherent double-scale pulses. An ANN model from TensorFlow software library [12] was employed to determine the FWHM of the ACF trace. The ANN is composed of three hidden layers with 32, 32, and 16 neurons. For the training of ANN, a dataset containing 13600 examples was used. To obtain data, we continuously changed the powers of both pumping diodes in the range from 4.5 to 0.5 W in the following order. At a fixed power of the LD1, we gradually reduced the power of the LD2 from 4.5 to 0.5 W with a step of 0.03 W and measured the parameters of the output radiation at each power step. Than the power of LD1 was reduced by 0.03 W, and the procedure was repeated until LD1 power became equal to 0.5 W. Eight parameters extracted from the DFT trace were used as features for an estimate: signal and Raman powers, spectral width of signal and Raman pulses, number and average power of the RF spectrum peaks, standard deviation, and normalized standard deviation of the RF peak power. Note that we were keeping only the variables showing a high correlation with the target characteristics. Instead of normalization of the features, we used a batch normalization layer before each nonlinear layer of the network. We also removed outliers in the outputs, corresponding to continuous-wave generation, unstable generation of fully stochastic radiation, and broken measurements. For this purpose, we filtered out examples with RF contrast less than 50 dB. This filtering process removed 30% of the initial data. The distribution of the ACF durations after filtration is shown in Fig. 2(a). The dataset was then divided randomly into training (80%) and testing (20%) sets. Part of the training set was used for model validation. The testing set was kept isolated from the rest during the training and optimization of the model. For ANN training, we employed the Adam optimization algorithm and mean squared error loss function commonly used for regression problems. To avoid overfitting, regularization and early stopping techniques were applied. After training the model, it was applied to the test set to predict durations of the ACF traces.

We found out that the model is able to predict the ACF duration with a mean absolute error near 3 ps or 4.8% mean absolute percentage error. Figure 2(b) shows the measured values compared to the predicted ones. Note that 69% and 89% of the testing samples were predicted with more than 5% and 10% relative error correspondingly. Only 3% of the testing data showed more than a 20% relative error.

The obtained results were also compared with the predictions of basic linear regression and an "Extreme Gradient Boosting" (XGBoost) machine learning technique [13], based on gradient boosting of regression trees [14]. The algorithm used the following parameters: the boosted tree number

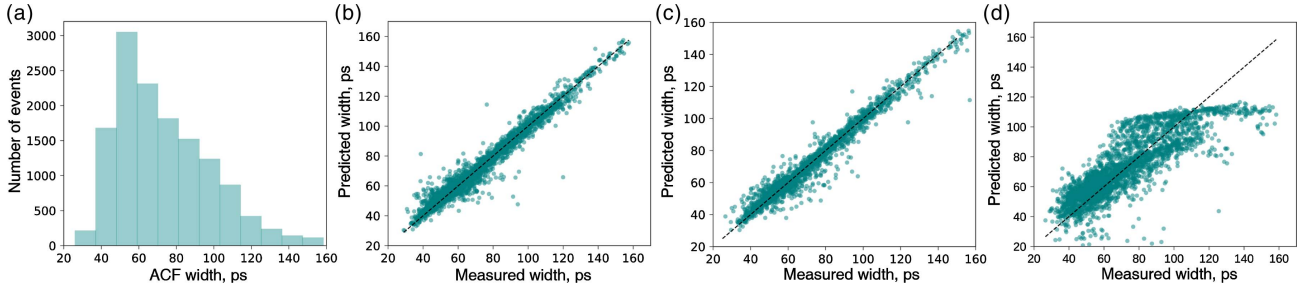

Fig. 2. (a) Distribution of the ACF durations. (b)–(d) Measured width of ACF traces compared to the predicted ones for the test set using the (b) neural network, (c) XGBRegressor, and (c) linear regression model.

Table 1. Mean Error of the Different Prediction Examples

Model	ACF Width	RF Contrast	Signal $\Delta\lambda$
ANN	4.8% (3.1 ps)	3.1% (1.9 dB)	5.8% (0.13 nm)
XGBoost	5% (3.2 ps)	3% (1.8 dB)	4.8% (0.11 nm)
Linear	15% (10.2 ps)	4% (2.3 dB)	14% (0.29 nm)

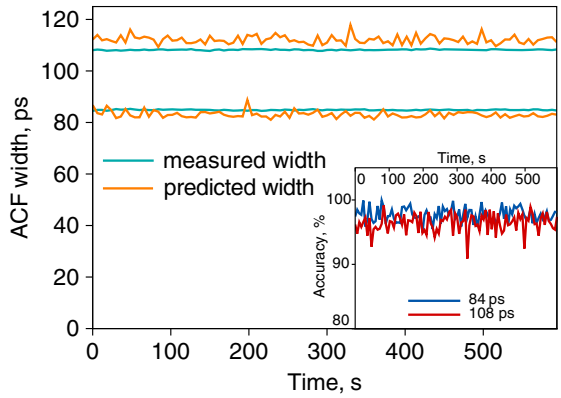

Fig. 3. Comparison of the measured and predicted ACF durations of the operating laser. Inset: accuracy of prediction.

(150), the maximum tree depth (7), and the learning rate (0.08). The linear model achieves only a 15% mean absolute percentage error, which confirms the nonlinearity of the problem. The quality of the prediction drops if the duration of the ACF trace exceeds 100 ps [Fig. 2(d)]. The XGBoost regression demonstrated ~5% average error, which is very close to the prediction results obtained with the neural network [Fig. 2(c)]. At the same time, XGBoost takes less time to be trained relative to an ANN and does not require rigorous parameter settings (number of hidden layers and neurons on each layer, learning rate, etc.). In our case, the difference between the XGBoost and ANN is not significant, and both methods performed well in solving the regression problem.

At the next stage, we tried to determine the other essential characteristics of the realized pulses such as the optical spectral width ($\Delta\lambda$) and RF beating spectra contrast before propagation in the fiber pool of the DFT measurement setup. It is worth noting that the same ANN architecture and parameters of XGBoost as those for ACF trace duration were used for prediction. The mean percentage and absolute errors of the different prediction examples obtained from each of the three models are summarized in Table 1. Therefore, the building models are able to make accurate predictions for the basic characteristics of the single-pulse generation regime of the F-8 laser.

Finally, the trained neural network was applied to operating the F-8 fiber laser. We the measured ACF of a pulsed regime and its DFT trace independently, and calculated the prediction accuracy of a pulse duration. The time series of the measured and predicted width of the ACFs, corresponding to the two mode-locked regimes with ~84 and ~108 ps output pulses, are shown in Fig. 3. Time fluctuations of the predicted width exceed the fluctuations of the measured width due to the difference in integration time of the autocorrelator and oscilloscope, and can be attributed to fluctuations of the pulse train at the laser output. The average error was maintained below 5% level during the whole measurement time (Fig. 3, inset). We tested our model on different pulsed regimes and made sure that predictions had the same degree of accuracy. Thus, the DFT analysis, in combination with machine learning algorithms, can be used for the control of the F-8 fiber laser operation, for example, for calculation of the objective functions of the pulsed regimes [15].

In conclusion, we demonstrated for the first time, to the best of our knowledge, a novel method for determination of a temporal duration of the mode-locked pulses using a DFT trace of a pulse comb and the machine learning technique. This method can be further improved, e.g., by more advanced filtering of the noisy and unstable signal generation regimes. Of course, different types of fiber lasers will generate pulses with different properties and distributions of key parameters. Their investigation will require new research efforts and adjusting of machine learning algorithms. However, the obtained results clearly show the feasibility of the accurate prediction of the basic pulse characteristics of the F-8 fiber laser, i.e., temporal width, optical spectrum, and RF spectrum using data extracted from the oscilloscope measurements. In other words, a single device could be used for resolving all key laser pulse parameters. Such a compact and robust measuring device can be a key component for the realization of a feedback loop in systems that require self-starting and self-optimization.

Funding. Russian Science Foundation (RSF) (17-72-30006).

REFERENCES

1. R. Iegorov, T. Teamir, G. Makey, and F. Ilday, Optica **3**, 1312 (2016).
2. J. Peng and S. Boscolo, Sci. Rep. **6**, 25995 (2016).
3. B. Nyushkov, S. Kobtsev, A. Komarov, K. Komarov, and A. Dmitriev, J. Opt. Soc. Am. B **35**, 2582 (2018).
4. S. Kobtsev, A. Ivanenko, A. Kokhanovskiy, and S. Smirnov, Laser Phys. Lett. **15**, 045102 (2018).
5. R. Woodward and E. Kelleher, Sci. Rep. **6**, 37616 (2016).
6. U. Andral, J. Buguet, R. S. Fodil, F. Amrani, F. Billard, E. Hertz, and P. Grelu, J. Opt. Soc. Am. B **33**, 825 (2016).
7. T. Baumeister, S. L. Brunton, and J. N. Kutz, J. Opt. Soc. Am. B **35**, 617 (2018).
8. C. A. Farfan, J. Epstein, and D. B. Turner, Opt. Lett. **43**, 5166 (2018).
9. R. Trebino, *Frequency-Resolved Optical Gating: The Measurement of Ultrashort Laser Pulses* (Springer, 2012).
10. A. Sanchez-Gonzalez, P. Micaelli, C. Olivier, T. Barillot, M. Ilchen, A. Lutman, A. Marinelli, T. Maxwell, A. Achner, M. Agåker, N. Berrah, C. Bostedt, J. D. Bozek, J. Buck, P. H. Bucksbaum, S. Carron Montero, B. Cooper, J. P. Cryan, M. Dong, R. Feifel, L. J. Frasinski, H. Fukuzawa, A. Galler, G. Hartmann, N. Hartmann, W. Helml, A. S. Johnson, A. Knie, A. O. Lindahl, J. Liu, K. Motomura, M. Mucke, C. O'Grady, J.-E. Rubensson, E. R. Simpson, R. J. Squibb, C. Såthe, K. Ueda, M. Vacher, D. J. Walke, V. Zhaunerchyk, R. N. Coffee, and J. P. Marangos, Nat. Commun. **8**, 15461 (2017).
11. K. Goda and B. Jalali, Nat. Photonics **7**, 102 (2013).
12. M. Abadi, P. Barham, J. Chen, Z. Chen, A. Davis, J. Dean, M. Devin, S. Ghemawat, G. Irving, M. Isard, M. Kudlur, J. Levenberg, R. Monga, S. Moore, D. G. Murray, B. Steiner, P. Tucker, V. Vasudevan, P. Warden, M. Wicke, Y. Yu, and X. Zheng, in *Operating Systems Design and Implementation* (2016), Vol. **16**, pp. 265–283.
13. T. Chen and C. Guestrin, in *22nd ACM SIGKDD International Conference on Knowledge Discovery and Data Mining* (ACM, 2016), pp. 785–794.
14. J. H. Friedman, *Annals of Statistics* (2001), pp. 1189–1232.
15. A. Kokhanovskiy, A. Ivanenko, S. Kobtsev, S. Smirnov, and S. Turitsyn, Sci. Rep. **9**, 2916 (2019).